

## Analytical Solution of Tapered Bimodular Beams

Dhafer Kh. Jadan  
Civil Engineering Department  
College of Engineering-University of Anbar  
Dhaferkj@yahoo.com

### ABSTRACT.

In this paper, an analytical solution of a tapered bimodular beam has been developed. An Euler-Bernoulli beam theory with shear deformations has been utilized to obtain the solution. The bimodular beams are different from those unimodular beams in having two different moduli of elasticity one in compression and another in tension. A verification for the solution has been performed using FEM analysis with ANSYS. The results of the program were very close the results of the analytical solution presented in this paper.

**KeyWords:** Tapered, Nonprismatic, Bimodular , beams.

### 1. INTRODUCTION.

The nonprismatic beams have been used in many civil and mechanical applications. Members of variable sections have a powerful significance in getting an optimum distribution of weight and strength and in some cases to satisfy architectural and functional requirements. From the most important applications of the nonprismatic members in engineering fields, are its use in highway bridges, aircraft structures and many other applications in civil and mechanical engineering.

In civil engineering construction, tapered elements offer the following advantages over "traditional" prismatic elements: (1) Weight economy, which is translated into longer or taller structures; (2) superior shear carrying performance, particularly at the supports and joints with other element, which is of vital importance in earthquake design; and (3) the bending moment and shear diagrams, which can correspond to the member's thickness, i.e., larger stiffness at the ends of the span reduces the positive moment due to gravity loads and increases the overall lateral stability and stiffness [1]

This is why the nonprismatic members have been gaining great importance in the recent decades.

The traditional scheme used in the analysis of nonprismatic beams is Euler -Bernoulli beam theory. Static analyses for tapered members are presented by many researchers, as shown in fairly complete lists in reference [2]. This reference states that the Euler -Bernoulli beam theory gives satisfactory results for beams with small tapering angles ( $15^\circ$  or less). This result is based on Lee [3] and Boley [4]. On the other hand, the shear analyses for tapering beams were studied by Chong *et al.* [5] and Schreyer [6]. The torsional problem was studied by Lee and Szabo [7]. The buckling problem was studied by Culver and Preg [8], Fogel and Ketter [9], and Gere and Carter [10]. Nonlinear bending of beams of variable cross section was studied by Verma and Murty [11]. Except special cases like Timoshenko and Young [12], Hibbeler [13] and Lee *at al.* [14], however, a lot of approximate and numerical solutions have been developed through the years. A straightforward early technique used to analyze a tapered beam is to divide it into a number of uniform elements, which is referred to as step representation, Wang CK. [15]. It has been well known that step representation is not efficient. Except for special cases like Timoshenko and Young [12], Hibbeler [13] and Lee *at al.* [14], no closed-form solution found for the analysis of the nonprismatic beams. This is why a lot of approximate and numerical solutions have been developed through the years.

Most of materials exhibit different tensile and compressive strains given the same stress applied in tension or compression. Classical theory of elasticity assumes that materials have the same elastic properties in tension and compression, but this is only a simplified model,

and does not account for material nonlinearities. Many studies have indicated that most materials, including concrete, ceramics, graphite, and some composites, exhibit different tensile and compressive strains given the same stress applied in tension or compression. Those materials which exhibit different elastic moduli in tension and compression are known as bimodular materials.

The elastic theory of bimodular solids was first proposed by Ambartsumyan [16], and Medri [17] by conducting experiments. Medri [17] reached the conclusion that the curve of stress-strain ( $\sigma - \varepsilon$ ) at the point of origin for materials with different moduli is nonlinear. Doong and Chen [18] developed a method for the analysis of different modulus problems based on an approximate trigonometric series. Zhang and Wang [19] proposed the finite element method for different moduli structures. Srinivasan and Ramachandra [20] applied a bimodulus finite element method to the calculation of large deflection of plates. Yang *et al.* [21] presented a method using the initial stress-finite element method for the analysis of bimodular structures. Tseng and Lee [22] used a finite strip method for the analysis of bimodular laminates. Ye [23] and Ye *et al.* [24] developed a finite element method in which variations of elastic modulus are different from that of Poisson's ratio. Tseng and Jiang [25] used the bimodulus theory to analyze the stress of laminated structure. Liu and Zhang [26] adopted the method of accelerating the convergence factor to increase the rate of convergence. Jun *et al.* [27] reviewed most of the major contributions to the solutions of problems with different moduli of elasticity. The shear formulae of the nonprismatic beam are based mainly on an approach used by Norris, Cited in Maki [28] and Timoshenko and Gere [29], where the author developed an approximate solution for the problem using the principles of strength of materials

In this paper, an analytical approach has been adopted to solve the problem of nonprismatic bimodular beams. This paper proceeds in a similar fashion but this time the problem of the nonprismatic beam is solved for a bimodular rather than unimodular beam. The results of this analytical solution have been compared with numerical results obtained from an FEM analysis using the famous commercial package ANSYS, and the results were found to be very close.

## 2. PROBLEM FORMULATION.

### 2.1 Bimodularity of the Beam.

Before discussing the bimodularity of the beam, the following assumptions and definitions must be mentioned first:

- 1- The material of the beam is homogenous anisotropic.
- 2- The fibers of the cross sections subjected to compression stress has a modulus of elasticity called  $E_n$  and the fibers subjected to a tensile stress has a different modulus of elasticity called  $E_p$  as shown in **Fig.( 3)**.
- 3- Straight planes of the cross sections of the beam before application the loads, remain plane after that application of the loads.
- 4- The stress-strain relationship is bilinear as shown in **Fig.( 1)**.

### 2.2 Neutral Axis Location.

This principle of determining the N.A. (abbreviated N.A) is that the forces normal to the face of the section must be balanced. Despite being this issue can be found in the literature concerning the bimodular beams, the author preferred to review this issue to simplify understanding next sections. Except the width of the beam,  $b$ , which is considered constant in this paper, all other sectional dimensions like  $h$ ,  $h_n$ ,  $h_p, y_1, \dots$  etc, are varied along the

beam and will be written as functions of  $x$  like  $h(x)$  in final form of each formula. Until the final formulae reached this notation will be ignored for simplicity.

For the section of the beam shown in Fig.(4)

$$\sum F_x = 0 \rightarrow \int_{-h_n}^{h_p} \sigma_x b dy_1 = \int_{-h_n}^{h_p} E \varepsilon_x b dy_1 = \int_{-h_n}^{h_p} E \frac{y_1}{\rho} b dy_1 = 0 \quad , \left( \varepsilon_x = \frac{y_1}{\rho} \right)$$

Simplifying more, then

$$\int_{-h_n}^0 E_n \frac{y_1}{\rho} b dy_1 + \int_0^{h_p} E_p \frac{y_1}{\rho} b dy_1 = 0$$

Combining this equation with the equation ( $h_p + h_n = h$ ) and solving those two algebraic equations simultaneously give

$$h_p(x) = \frac{\sqrt{E_n}}{\sqrt{E_n} + \sqrt{E_p}} h(x) \quad \text{and} \quad h_n(x) = \frac{\sqrt{E_p}}{\sqrt{E_n} + \sqrt{E_p}} h(x) \quad (1)$$

These quantities will be altered in position in the case of negative bending moment, the tensile stresses will be above the N.A. and the compressive stresses will be below the N.A. .

Those heights  $h_p$  ,  $h_n$  ,  $h$  from now on will be written  $h_{p(x)}$  ,  $h_{n(x)}$  ,  $h(x)$  indicating that those heights are at a distance ( $x$ ) from one end of the beam. Hence the values of  $h_{p(x)}$  and ,  $h_{n(x)}$  will be varied along the beam. If the nonprismatic beam was a tapered one, then the values of the  $h_{p(x)}$  and  $h_{n(x)}$  will be as depicted in **Fig.( 3)**

### 2.3 Bending Stresses.

As pointed out in the introduction, the reference (Johnston 1976) [2] states that the Euler-Bernoulli beam theory gives satisfactory results for beams with small tapering angles ( $15^\circ$  or less). This result is based on Lee [3] and Boley [4]. In addition, the problem of the cantilever wedge (**Fig.( 3)**) has been solved using theory of elasticity (Timoshenko and Gere [29]). It was found in this solution that for the values of the angle of taper ( $\alpha$ ) equal to  $0^\circ$  ,  $5^\circ$  ,  $10^\circ$  ,  $15^\circ$  ,  $20^\circ$  and  $20^\circ$  , the error behind using the traditional Bernoulli-Euler formula for flexural stresses is  $0\%$  ,  $0\%$  ,  $3\%$  ,  $5\%$  and  $10\%$ .

And being most of the tapered beams in engineering practice almost have tapering angle less than  $15^\circ$  , the traditional flexure formula based on Bernoulli-Euler beam theory, will be adopted here in this paper for the nonprismatic beam but of course with variable depth. Later on, in the next sections a comparison with an FEM analysis will be taken to see the reliability of this theory for the nonprismatic beams.

Taking sum of moments about N.A. equals zero, yields

$$\sum M_{N.A.} = M(x) \rightarrow \int_{-h_n}^{h_p} \sigma_x b y_1 dy_1 = \int_{-h_n}^{h_p} E \varepsilon_x b y_1 dy_1 = \int_{-h_n}^{h_p} E \frac{y_1^2}{\rho} b dy_1 = M(x) \quad (2)$$

Simplifying more, then

$$\int_{-h_n}^0 E_n \frac{y_1^2}{\rho} b dy_1 + \int_0^{h_p} E_p \frac{y_1^2}{\rho} b dy_1 = M(x)$$

Rearranging this equation and making use of Equation (1), yields

$$\frac{1}{\rho} = \frac{-M(x)}{E_r I} \quad (3)$$

The negative sign has been added to the equation so that the positive bending moment will produce negative curvature according to the coordinate system adopted in paper.

Where:

$I = \frac{bh^3}{12}$  : moment of inertia of the cross section of the beam about the centroidal axis at a

distance (x) from one end of the beam ,and

$E_r$ : reduced modulus of elasticity for bimodular beams which equals to

$$E_r = \frac{4E_p E_n}{(\sqrt{E_p} + \sqrt{E_n})^2} \quad (4)$$

For a unimodular section ( $E_n=E_p=E$ ) and by direct substitution in Equation (4) gives  $E_r=E$ .

The normal bending stress at any fibre within the cross section can be found using the flexure formulae with

$$\begin{aligned} \sigma_p(x) &= E_p \varepsilon_x = E_p \frac{y_1}{\rho} = E_p \frac{y_1 M}{E_r I} = \frac{M y_1}{I} \cdot \frac{E_p}{E_r} \\ \sigma_n(x) &= E_n \varepsilon_x = E_n \frac{y_1}{\rho} = E_n \frac{y_1 M}{E_r I} = \frac{M y_1}{I} \cdot \frac{E_n}{E_r} \end{aligned} \quad (5)$$

Where

$\sigma_p(x)$  : the tensile normal stresses.

$\sigma_n(x)$  : the compressive normal stress, and

$y_1$ : a depth measured from the N.A. along the cross section.

## 2.4 Shear Stresses

In same problem of the cantilever wedge stated in the previous section, it was found in this solution that for the values of the angle of taper ( $\alpha$ ) equal to  $0^\circ$ ,  $5^\circ$ ,  $10^\circ$ ,  $15^\circ$ ,  $20^\circ$  and  $20^\circ$ , the error due to using the traditional Euler-Bernoulli formula in deriving shear stresses was 50%, 50%, 48%, 47% and 45%. So the using of the traditional shear formula ( $\tau = \frac{VQ}{I b}$ )

gives very misleading results when applied to nonprismatic beams.

Hence it's important to seek an alternative solution that is more accurate than this formula even if the new solution was an approximate solution. The new solution is an approximate one, because it depends on Bernoulli-Euler theory which is in turn gives an approximate solution for the nonprismatic beams as illustrated in the previous section.

The derivation of shear formulae will be separated into three parts:

- 1- The shear formula at the fibers where the flexure stresses are tensile stresses.
- 2- The shear formula at the fibers where the flexure stresses are compressive stresses.
- 3- The shear formula at the N.A.

Beside that and as mentioned in section 2.2, due to the altering in position for ( $h_p$ ) and ( $h_n$ ) in the case of negative bending moment, all the above three cases will be treated firstly for positive bending moment and then will be retreated again for the negative bending moment.

### 2.4.1 Positive Bending Moment.

For the case  $r = \frac{E_p}{E_n} < 1$ , refer to the element at a distance ( $x$ ) from one end of the beam as in Figs.( 3 and 5). Then for a fiber lies at a depth ( $y_1$ ) below the (N.A.) where the flexure stresses are tensile stresses

$$\sum F_x = 0 \rightarrow$$

$$\rightarrow \int_{y_1}^{h_{p1}} \sigma_p(x) b dy + \tau b dx - \int_{y_2}^{h_{p2}} \sigma_p(x+dx) b dy = 0$$

$$\rightarrow \int_{y_1}^{h_{p1}} \frac{M(x)y_1}{I_1} \cdot \frac{E_p}{E_r} b dy_1 + \tau b dx - \int_{y_2}^{h_{p2}} \frac{M(x+dx)y_2}{I_2} \cdot \frac{E_p}{E_r} b dy_2 = 0 \quad (6)$$

Where

$I_1$  and  $I_2$  are the moments of inertia of the cross section at distances ( $x$ ) and ( $x+dx$ ) from one end of the beam.

Noting the following:

$$M(x+dx) = M(x) + \frac{dM(x)}{dx} dx$$

$$V(x) = \frac{dM(x)}{dx} \text{ is the shear force.}$$

$y_2 = y_1 + S dx$  and  $S$ : is the slope of the N.A. and its value can be calculated as follows

$$S = \frac{h_{p2} - 0.5h_2 - (h_{p1} - 0.5h_1)}{dx}$$

From Equation (1), substitute the expressions for ( $h_{p1}$  and  $h_{p2}$ ) and simplifying then

$$S = \frac{1 - \sqrt{r}}{2(1 + \sqrt{r})} \frac{dh}{dx} \quad (7)$$

Where:  $r = \frac{E_p}{E_n}$  the modular ratio.

The same value would be obtained for ( $S$ ) if the Equation (7) is written in terms of ( $h_n$ ). As the slope of the taper is constant, the slope of the N.A. is also constant as it clear from Equation (7).

The moment of inertia at a distance ( $x+dx$ ) may be calculated as follows

$$I_2 = \frac{b h_2^3}{12} = \frac{b (h_1 + dh)^3}{12}$$

Substituting the expressions for ( $I_1$ ,  $I_2$ ,  $V(x)$ ,  $y_2$  and  $S$ ) into Equation (7), neglecting all higher powers and product terms of infinitesimals, simplifying and rearranging, yields

$$\tau = \frac{V(x) Q_p}{I_1 b} + \frac{M(x) h}{4 I_1} \left( 1 - \frac{Q_p h(x)}{I_1} \right) \frac{dh}{dx} - \frac{M(x) S}{I_1} \frac{E_p}{E_r} y_1$$

Where:

$$Q_p = \frac{E_p}{E_r} \int_{y_1}^{h_{p1}} y_1 \cdot dy_1 = \frac{b}{2} \left( \frac{h^2}{4} - y_1^2 \frac{E_p}{E_r} \right) \quad (8)$$

Now, the subscript used in ( $I_1$ ) is no longer needed and can be dropped. The final form of the shear formula for any fiber below the N.A. at a distance ( $x$ ) from one end of the beam is

$$\tau = \frac{V(x)Q_p}{I(x)b} + \frac{M(x)h}{4I(x)} \left( 1 - \frac{Q_p h(x)}{I(x)} \right) \frac{dh}{dx} - \frac{M(x)S}{I(x)} \frac{E_p}{E_r} y_1(x) \quad (9)$$

$\tau_p(x)$  is the shear stress where the flexure stresses are tensile stresses.

By investigating this equation, it's important to note the following:

1-The first term represents the shear stress in a prismatic beam, but this time for a bimodular beam and this arises in the quantity ( $Q_p$ ).

2- The second term represents the effect of tapering on the shear stresses. This term is the same as in the equation derived by Norris for shear stresses (Cited in MAKI [28] and Timoshenko and Gere [29]). Again the effect of bimodular ratio appears in the quantity ( $Q_p$ ) in this term.

3- The third term represents the effect of the bimodular ratio on the shear stresses. This could be seen in the quantity ( $S$ ) which is the slope of the N.A. (Equation (7)).

Now, to derive a formula for the shear stress above the N.A where the flexure stresses are tensile stresses and for the case  $r = \frac{E_p}{E_n} < 1$ , refer to the element at a distance ( $x$ ) from one end of the beam as in Figs.( 3 and 6). Then for a fiber lies at a depth ( $y_3$ ) above the (N.A.)

$$\sum F_x = 0 \rightarrow$$

$$\int_{-h_{n1}}^{-y_3} \sigma_n(x) b dy + \tau b dx - \int_{-h_{n2}}^{-y_4} \sigma_n(x+dx) b dy = 0$$

$$\rightarrow \int_{-h_{n1}}^{-y_3} \frac{M(x)(y_3)}{I_1} \cdot \frac{E_n}{E_r} b dy_3 + \tau b dx - \int_{-h_{n2}}^{-y_4} \frac{M(x+dx)(y_4)}{I_2} \cdot \frac{E_p}{E_r} b dy_4 = 0$$

$y_4$  can be transformed into  $y_3$  from the following relation

$$y_4 = y_3 - S dx \quad (10)$$

Proceeding in the same way of deriving Equation (9), the following equation will be obtained

$$\tau_n(x) = \frac{V(x)Q_n}{I_1 b} + \frac{M(x)h}{4I_1} \left( 1 - \frac{Q_n h(x)}{I_1} \right) \frac{dh}{dx} - \frac{M(x)S}{I_1} \frac{E_n}{E_r} y_3$$

Unifying the depths of the fibers above and below the N.A. by one notation, say ( $y_1$ ), the above equation can be written as follows

$$\tau_n(x) = \frac{V(x)Q_n}{I(x) b} + \frac{M(x)h(x)}{4I(x)} \left( 1 - \frac{Q_n h(x)}{I(x)} \right) \frac{dh}{dx} - \frac{M(x)S}{I(x)} \frac{E_n}{E_r} y_1(x) \quad (11)$$

Where

$\tau_n(x)$ :  $\tau_p(x)$  is the shear stress where the flexure stresses are compressive stresses, and  $Q_n$  is defined as

$$Q_n = \frac{E_n}{E_r} \int_{-h_n}^{-y_1} y_1 \cdot dy_1 = \frac{b}{2} \left( \frac{h^2}{4} - y_1^2 \frac{E_n}{E_r} \right) \quad (12)$$

Finally the shear stress at any section passes through the N.A. will be can be calculated using Equation (9) or Equation (11) with ( $y_1 = 0$ ), which leads to

$$\tau_{N.A.}(x) = \frac{3V(x)}{2bh_{(x)}} - \frac{3M(x)}{2bh_{(x)}^2} \frac{dh}{dx} \quad (13)$$

The preceding derivations for the shear stresses are based on the case of ( $E_p < E_n$ ).

For the case ( $r = \frac{E_p}{E_n} > 1$ ), the state of stresses will be for positive moments as in **Fig.( 7)**.

One may go through the same procedure that leads to shear stress formulae for the case of  $r < 1$  in positive moment, to get the shear stress formulae for the case  $r > 1$  and also in positive bending moment, and the result is that the same Equations (9,11 and 13) was obtained for the shear stresses of this case.(that is for  $r > 1$ ).

#### 2.4.2 Negative Bending Moment.

The case of negative bending moment is depicted in **Fig.(8)**.

The shear stress derivation for this case is similar to the case when the bending moment is positive, except being the tensile stresses is above the N.A. and the compressive stresses is below the N.A. while the formulae for shear stresses are the same for the fibers above and below the N.A. except the difference in the modulus of elasticity, hence the same formulae described in Equations (9, 11 and 13) will be used to find the shear stress in the case of negative bending moment.

#### 2.5.1 Transformation of the coordinate $y_1$ .

The ( $y_1$ ) coordinate used in all the preceding flexure and shear stress formulae in this paper was measured from the N.A.. Being the N.A. is linearly varied along the beam, makes it more convenient to measure the ( $y$ ) coordinate from the ( $x$ ) axis. Hence a transformation formula will now be prepared for this purpose as follows:

1- Zones of positive bending moment.

a- If ( $r < 1$ ) then as explained in sections 2.4, the N.A. will be as shown in **Fig.( 9)**.

$$y_1 = y + \frac{h}{2} - h_n \quad (14)$$

Substituting the value of ( $h_n$ ) from Equation (1) into Equation (14), then

By simplifying and remembering that  $r = \frac{E_p}{E_n}$ , yields

$$y_1(x) = y_{(x)} + \frac{1 - \sqrt{r}}{2(1 + \sqrt{r})} h_{(x)} \quad (15)$$

b- If ( $r > 1$ ) then as shown in **Fig.( 10)** and as known from section 2.4

In a similar fashion discussed in the item a, then

$$y_1(x) = y_{(x)} + \frac{1 - \sqrt{r}}{2(1 + \sqrt{r})} h_{(x)} \quad (16)$$

1- Zones of Negative bending moment.

a- If ( $r < 1$ ) then as explained in sections 2.4, the N.A. will be as shown in **Fig.( 11)**. Proceeding with the same procedure discussed for the positive moment, then

$$y_1(x) = y_{(x)} - \frac{1 - \sqrt{r}}{2(1 + \sqrt{r})} h_{(x)} \quad (17)$$

b- If ( $r < 1$ ) then as shown in **Fig.( 12)** and as known from section 2.4, and just like the previous cases the following relation may be obtained.

$$y(x)_1 = y_{(x)} - \frac{1 - \sqrt{r}}{2(1 + \sqrt{r})} h_{(x)} \quad (18)$$

### 2.6.1 Flexural Deformations.

The flexural deformations considered in this paper are small deformations. Hence the curvature in Equation (3) is

$$\frac{1}{\rho} = \frac{d_2 v_f}{dx^2} \quad (18)$$

And this formula can found in many elementary calculus books.

Where

$v_f$  : flexural deformations

Then Equations (3 and 18) will lead to

$$\frac{d_2 v_f}{dx^2} = - \frac{M(x)}{E_r I_{(x)}} \quad (19)$$

And from this equation and by two successive integrations and applying the boundary conditions, the flexural deformations can be obtained.

### 2.6.2 Shear Deformations.

According to Timoshenko's beam theory, the transverse deformations are not only bending deformations (those discussed in the proceeding sections) but also shear deformations and the latter will be discussed in this section for bimodular beams. According to Timoshenko's beam theory, plane sections in beams will no longer remain plane sections when shear deformations are considered, but they will be curved as shown in **Fig.( 13)** which shows a deformed element in a beam due to shear stresses only.

Shear deformations may be obtained by considering the slope of the deflected curve at the N.A. (as shown in **Fig.( 13)** which is equal to  $\gamma_c = \frac{dv_s}{dx}$ ,

Where  $v_s$  is shear deflection at the N.A.,

$\gamma_c$  : shear strain at the N.A. which equals the shear stress divided by the modulus of elasticity in shear.

Now, integrating this equation will lead to the shear deformations. But using this method to find the shear deformations is not accurate for two reasons:

- 1- The deflection is based upon shear strains at the N.A. and neglects the shear variation throughout the section.
- 2- The deflection is based upon pure bending theory only.

The second defect can be removed by using a more exact approach like theory of elasticity. The first defect can be removed by using the principle of virtual work (Timoshenko and Gere [29]).

Hence the principle of virtual work (specifically unit load method) will be utilized in this paper to obtain the shear deformations. The equation that yields when applying the virtual work method

$$v_s = \int V_u \cdot d\lambda \quad (20)$$

Where

$v_s$  transverse shear displacement caused by real shear forces,

$V_u$  virtual shear forces resulting from application of a unit load in the direction of  $v_s$ .

$d\lambda$  differential of real shear displacement caused by real loads.

Refer to **Fig.(14)**

$$V_u = \tau_u \cdot dydz \quad \text{and} \quad d\lambda = \gamma dx$$

$$dv_s = (\tau \cdot dydz) \cdot (\gamma dx)$$

Then Equation (20) will become

$$v_s = \int \tau_u \cdot \frac{\tau_l}{G} dx dy dz \quad (21)$$

$\tau_l$  : Shear stress due to real loads.

$\tau_u$  : Shear stress due to virtual unit load in the direction of  $v_s$ .

Since there are two moduli of elasticity in flexure, one in tension ( $E_p$ ) and one in compression ( $E_c$ ), then there are two moduli of elasticity in shear, one in tension and one in compression. From reviewing the literature (Jun *et. al.* [27]), it was found that many researchers proposed different formulae for the modulus of elasticity in shear. Those proposals are not based on rigorous analysis rather than suggestions dependent mainly on the researchers' intuition. In addition those formulae when used to obtain the shear deformations for bimodular beams, they do not lead to the traditional formulae for unimodular beams when the beam considered as unimodular. For all this, the author suggests the following value for ( $G$ ) to be used in Equation (21)

$$G_r = \frac{E_r}{2(1+\nu)} \quad (22)$$

Where:

$G_r$  : the reduced shear modulus of elasticity (reduced because its value is always less than  $G$  for unimodular beam).

The author adopted Equation (22) because the flexural analysis of the bimodular beam led to the use of the traditional flexural formula, Equation (3), but this time with the reduced modulus of elasticity  $E_r$ , a fact that inspired the use of Poisson's relation with  $E_r$ . Later this will show reasonable results when compared with FEM analysis. In addition, when the section is unimodular section then  $E_r$  and the value of  $E_p = E_c = E$  in Equation (22) leads to the value  $G$  which is the value of shear modulus for a unimodular beam.

### 2.7 Application Example.

The application example will be a cantilever loaded with a concentrated load at the free end as shown in Fig.( 15).

In this example the flexural and shear stresses in addition to the flexural and shear deformations will be calculated. Before proceeding with the calculations, the following basic quantities will be calculated first.

$$\text{If } \gamma = \frac{h_e - h_o}{h_o} \text{ then } \gamma = \frac{3h_o - h_o}{h_o} = 2$$

$$h(x) = h_o + \frac{dh}{dx}x = h_o + \frac{h_e - h_o}{l}x = h_o(1 + \frac{h_e - h_o}{lh_o}x) = h_o(1 + \frac{\gamma}{l}x) = h_o(1 + \frac{2}{l}x)$$

$$\frac{dh}{dx} = \frac{2h_o}{l} \text{ also } I(x) = \frac{bh^3}{12} = \frac{bh_o^3}{12}(1 + \frac{\gamma}{l}x)^3 = I_o(1 + \frac{2}{l}x)^3 \text{ where } I_o = \frac{bh_o^3}{12}$$

$$M(x) = P.x \text{ and } V(x) = P$$

When the following given values for  $h_o = 0.25m, l = 3m, P = 100kN$  are used in above basic relations and in the equations of sections (2.3 and 2.4), the following results will be obtained.

#### 2.7.1 Flexural deformations.

As mentioned in section 2.5, the flexural deformations can be calculated from Equation (19)

$$\frac{d^2v_f}{dx^2} = -\frac{M(x)}{E_r I} = \frac{-Px}{E_r I_o(1 + \frac{2x}{l})^3} \quad (23)$$

In the above formula, the expression of the moment of inertia has been defined using ( $h_o, h_e$  and  $l$ ) because this will simplify the next expressions.

Integrating Equation (23) twice and imposing the boundary conditions, which, for the cantilever example in this research are

$$v_f = 0 \quad @ \quad x = l$$

$$\frac{dv_f}{dx} = 0 \quad @ \quad x = l$$

This will leads to the following deflection equation

$$v_f = -\frac{Pl^3 \ln(l+2x)}{8E_r I_o} - \frac{Pl^4}{16E_r I_o(l+2x)} + c1x + c2$$

Where:  $c1$  and  $c2$  are constants, and their values are as follows

$$c1 = \frac{5Pl^2}{72E_r I_o} \quad \& \quad c2 = \frac{Pl^3(-7+18\ln(3l))}{144E_r I_o}$$

#### 2.7.2 Shear deformations.

From Equation (21), the shear deformation using unit load method is

$$v_s = \int_V \tau_u \cdot \frac{\tau_l}{G_r} dx dy dz$$

And this equation can be written as

$$v_s = \frac{b}{G_r} \int_{x_1}^l \left( \int_0^{h_p} \tau_{pu} \cdot \tau_{pl} dy + \int_{-h_n}^0 \tau_{nu} \cdot \tau_{nl} dy \right) dx \quad (24)$$

Where

$\tau_{pu}$ ,  $\tau_{nu}$  the shear stress due to unit load applied in the direction of the required displacement, as defined in Equations (9 and 11) respectively, with  $M(x) = 1 \cdot x$  and  $V(x) = 1$   
 $\tau_{pl}$ ,  $\tau_{nl}$  the shear stress due to real load applied, taken from Equations (9 and 11) respectively with  $M(x) = P \cdot x$  and  $V(x) = P$ .

The expressions for,  $G_r$ ,  $h_p$  and  $h_n$  are taken from Equations 22, 1 and 2) respectively.

The integration of the Equation (24) started from the point  $x_1$  and not from zero because the moment and the shear force due to unit load at distance ( $x_1$ ), from the free end until this point are zeros. Hence this formula will determine the shear displacement at the point ( $x_1$ ).

The results of the shear displacements are so long that it could not be expressed symbolically here symbolically. Hence these results will be obtained and presented numerically for each case of the example presented in this section.

For all the graphs presented in this research the quantity ( $y/l$ ) is the ratio of the distance from the N.A. to a specific depth of the section, while the quantity ( $x/l$ ) is the ratio of a distance from the free end to the length of the beam.

### 3. CONCLUSIONS.

As mentioned in the introduction, most of materials exhibit different moduli in compression and in tension. The ratio between those moduli is called the modular ratio. The modular ratio for some materials like steel approaches unity, but for others it is not. This will result in different stresses and deformations according to the modular ratio. The quantities  $\frac{E_p}{E_r}$  and

$\frac{E_n}{E_r}$  which is mentioned in the formulae of the stresses and deformations, Equations (5, 9, 11, 19 and 21), by simple simplification, it can be shown that these quantities is equal to  $\frac{(1+\sqrt{r})^2}{4}$  and  $\frac{(1+\sqrt{r})^2}{4r}$  respectively. Hence the flexural and shear stresses in a bimodular

beam is not depending on the modulus in tension or in compression alone rather than on the ratio between them, that is the modular ratio ( $r = \frac{E_p}{E_n}$ ). This is why the graphs and the tables

for the flexural and shear stresses and the flexural and shear deformations at a specific section are varying with the modular ratios. The more important of that is that the material for a specific loadings and dimensions would have different stresses and deformations according to the modular ratio of that material. From this one could see the importance of the bimodular analysis over the unimodular analysis (considering one modulus of elasticity). To see this point in a specific application, the cantilever beam studied in this paper has been analyzed as a bimodular beam with different values of the modular ratio and another time as a unimodular beam with one modulus of elasticity equals to the average of the two moduli of the beam. The differences between the two approaches of the analysis in stresses and deformations are listed in table 5. This difference is significant and cannot be ignored for large and small modular ratios. These differences in results are also depicted graphically in **Figs.( 16 to 25)**. The shear

stresses are not having the maximum values at the N.A. within the section anymore but in most cases occur at the taper as shown in **Tables (3 and 4)** and the **Figs.( 16 to 21)** except at the locations where the bending moment is zero like the free end of a cantilever beam. Being the maximum shear stress in bimodular tapered beam occurs mostly at the taper is due to the tapering in the beam and the modular ratio. The contribution of the tapering is found in the second and third terms of the shear stress formulae, Equations (9 and 11). This contribution is represented by the slope of the taper ( $\frac{dh}{dx}$ ) which is stated explicitly in the second term and implicitly in the third term because the slope of the N.A. ( $S$ ) is depending partially on the slope of the taper (refer to Equation (7)). The contribution of the modular ratio is found in the three terms of Equations (9 and 11) and represented by the quantity  $\frac{E_p}{E_r}$  which in turn is stated implicitly in the quantity ( $Q_n$ ). In the third term this contribution is found in the slope of the N.A. ( $S$ ). The reduced modulus of elasticity  $E_r$ , Equation (4) can be written as

$E_r = \frac{4E_p}{(1+\sqrt{r})^2}$ , hence the flexural displacement formula, Equation (19) and the shear

displacement formula, Equations (21 and 22) will have larger values for the larger modular ratios and vice versa. This is depicted graphically in **Figs.( 25)**. The solution of the bimodular material problems establishes more accurate theoretical solution for the composite materials which have full interaction. The accuracy of the solution has been established by comparing the solution with the solution of the finite element method using the well known commercial package Ansys. **Table (6)** lists maximum errors in the paper solution in comparison with the solution of the FEM. Maximum error in flexure deformation was 0.06% that in shear stress was 2.3% and that in deformation was 2.0 %. Hence the solution has a good accuracy in the view of the structural analysis. Those are can be interpreted by noting that the compatibility of the deformations and the stresses was not considered in the solution.

Beside that the vertical stresses have been ignored. This is regarding the paper solution. Concerning the FEM, the analysis was not conducted to different meshing in size to establish the stability and accuracy of the solution. This could be returned to being the errors were relatively very small and accepted. Finally **Fig.(28)** shows the shear stresses distribution which is different from that for the prismatic and even from that for the unimodular tapered beam.

#### 4. REFERENCES.

- [1] J. Dario Aristizabal-Ochoa "Tapered Beam And Column Elements In Unbraced Frame Structures" J. of Computing in Civil Engineering, Vol. 1, No. 1, p 1. (1987).
- [2] Johnston, B. G. Guide to stability design criteria for metal structures, Chap.11. Tapered structural members, 3rd Ed., John Wiley & Sons, Inc., New York, N.Y., 330-358. (1976).
- [3] Lee, L. H. N. "On the lateral buckling of a tapered narrow rectangular beam." J. Appl. Mech., 26, 457-458. (1959).
- [4] Boley, B. A. "On the accuracy of the Bernoulli-Euler theory of beams of variable section. " J. Appl. Mech., 30(3), 373-378. (1963).
- [5] Chong, K. P., Swanson, W. D., and Matlock, R. B. "Shear analysis of tapered beams." . Struct. Div., ASCE, 102(9), 1781-1788. (1977).
- [6] Schreyer, H. L. "Elementary theory for linearly tapered beams." / . Eng. Mech. Div., ASCE, 104(3), 515-527. (1978).
- [7] Lee, G. C, and Szabo, B. A. "Torsional response of tapered I-girders." J.Struct. Div.,

- ASCE, 93(5), 233-252. . (1967).
- [8] Culver, C. G., and Preg, S. M. "Elastic stability of tapered beam-columns." J. Struct. Div., ASCE, 94(2), 455-470. (1968).
- [9] Fogel, C. M., and Ketter, R. L. "Elastic strength of tapered columns." J. Struct. Div., ASCE, 88(5), 67-106. (1962).
- [10] Gere, J. M., and Carter, W. O. "Critical buckling loads for tapered columns." J. Struct. Div., ASCE, 88(1), 1-11. (1962).
- [11] Verma, M. K., and Murty, A. V. K. "Non-linear bending of beams of variable cross-section." Int. J. Mech. Sci., 15, 183-187. . (1973).
- [12] Timoshenko, S. P., and Young, D. H. Theory of structures, 2<sup>nd</sup> Ed., MacGraw-Hill, Inc., New York, N.Y. (1965).
- [13] Hibbeler, R. Structural analysis, 2<sup>nd</sup> Ed., Macmillan publishing Co., New York, N.Y. . (1990).
- [14] Lee, S. Y., Ke, H. Y., and Kuo, Y.H. "Exact static deflection of a non-uniform Bernoulli-Euler beam with general elastic end restraints." Comp. And Struc. 36(1), 91-97. (1990).
- [15] Wang CK. Stability of rigid frames with nonuniform members. J of Struc Divi.;93(1) :275–94. (1967).
- [16] Ambartsumyan, S. A. "Elasticity theory of different modulus, W. Ruifeng and Z. Yunzhen, eds., China Railway Press, Beijing, 11–32. (1982).
- [17] Medri, G. "A nonlinear elastic model for isotropic materials with different behaviour in tension and compression." Trans. ASME, J. Appl. Mech., 104\_26\_, 26–28. . (1982).
- [18] Doong, J. L., and Chen, L. W. "Axisymmetric vibration of an initially stressed bimodulus thick circular plate." J. Sound Vib., 94, 461–468. (1984).
- [19] Zhang, Y., and Wang, Z. "The finite element method for elasticity with different moduli in tension and compression." J. Comput. Struct. Mech. Appl., 1\_6\_, 236–246. (1989).
- [20] Srinivasan, R. S., and Ramachandra, L. S. "Large deflection analysis of bimodulus annular and circular plates using finite elements." Comput. Struct., 31\_5\_, 681–691. . (1989).
- [21] Yang, H., Wu, R., Yang, K., and Zhang, Y. "Solve bimodulus problem by using initial stress." J. Dalian Univ. Technol., 32\_1\_, 35–39. (1992).
- [22] Tseng, Y.-p., and Lee, C.-T. "Bending analysis of bimodular laminates using a higher-order finite strip method." Compos. Struct. 30, 341–350. (1995).
- [23] Ye, Z. "A new finite element formulation for planar elastic deformation." Int. J. Numer. Methods Eng., 14\_40\_, 2579–2592. (1997).
- [24] Ye, Z., Yu, H., and Yao, W. "A finite element formulation for different Young's modulus when tension and compression loading." Proc., Conf. on Computational Mathematics, Pohang Univ. of Science and Technology, Pohang, South Korea, 2–5. (2001).
- [25] Tseng, Y.-p., and Jiang, Y.-c. "Stress analysis of bimodular laminates using hybrid stress plate elements." Int. J. Solids Struct. 35\_17\_, 2025–2028. . (1998).
- [26] Liu, X., and Zhang, Y. "Modulus of elasticity in shear and accelerate convergence of different extension—Compression elastic modulus finite element method." J. Dalian Univ. Technol., 40, 527–530. (2000).
- [27] Jun-yi Sun, Hai-qiao Zhu, Shi-hong Qin, Da-lin Yang and Xiao-ting He. "A review on the research of mechanical problems with different moduli in tension and compression" J of Mechanical Science and Technology, 24 (9) 1845–1854. (2010).
- [28] Maki A.C., Kuenzi E.W. "Deflection and Stresses of Tapered Wood Beams". Research

paper FPL 34. Madison, WI., U.S. Department of Agriculture, Forest Service, Forest Products Laboratory. . (1965).

- [29] Timoshenko, S. P. and Gere, J. M., “Mechanics of Materials”, 3<sup>rd</sup> Edition, Van Nostrand Reinhold Company Ltd., London. (1973).

**Table (1):** Shear Deformations along the beam for different bimodular ratios (mm).

$r$	$x / l$	
	0	0.25
0.25	0.110	0.075
0.5	0.212	0.135
1.0	0.336	0.214
2.0	0.425	0.270
3.0	0.440	0.285

**Table (2):** Flexural Deformations along the beam for different bimodular ratios (mm).

$r$	$x / l$			
	0	0.25	0.5	0.75
0.25	20.22	10.59	4.28	0.97
0.5	26.19	13.72	5.54	1.26
1.0	35.95	18.83	7.60	1.73
2.0	52.39	27.43	11.08	2.52
3.0	67.09	35.13	14.19	3.23

**Table (3):** Flexural Stresses at Taper (MPa).

$r$	$x / l$							
	0.25		0.5		0.75		1.0	
	Tensile	Compressive	Tensile	Compressive	Tensile	Compressive	Tensile	Compressive
0.25	25.00	-50.00	28.12	-56.26	27.00	-54.00	25.00	-50.00
0.5	28.46	-40.24	32.00	-45.26	30.72	-43.46	28.46	-40.24
1.0	33.34	-33.34	37.50	-37.5	36.00	-36.00	33.34	-33.34
2.0	40.24	-28.46	45.26	-32.00	43.46	-30.72	40.24	-28.46
3.0	45.54	-26.28	51.22	-29.56	49.18	-28.40	45.54	-26.28

**Table (4):** Shear stresses at Taper, above and below N.A. (MPa).

$r$	$x / l$					
	1/4		1/2		3/4	
	Below N.A.	Above N.A.	Below N.A.	Above N.A.	Below N.A.	Above N.A.
0.25	-1.25	-2.50	-1.41	-2.81	-1.35	-2.70
0.5	-1.42	-2.01	-1.60	-2.26	-1.53	-2.17
1.0	-1.67	-1.67	-1.88	-1.88	-1.80	-1.80
2.0	-2.01	-1.42	-2.26	-1.60	-2.17	-1.54
3.0	-2.28	-1.31	-2.82	-1.34	-2.80	-1.24

**Table (5):** Comparison between Bimodular and Unimodular Analysis (with  $E_{ave}$  using an FEM analysis).

$r$	$E_p$ (MPa)	$E_n$ (MPa)	$E_{ave}=(E_p+E_n) / 2$ (MPa)	Difference % in Max.Flexural Deformation	Difference % in Max.Flexural Stresses	Difference % in Max.Sheer Stresses
0.25	35000	140000.0	87500.0	28.0	33.3	33.3
0.5	35000	70000.0	52500.0	7.3	17.1	17.0
1.0	35000	35000.0	35000.0	1.3	0.0	0.3
2.0	35000	17500.0	26250.0	7.3	13.7	17.0
3.0	35000	11666.7	23333.3	18.6	26.8	33.5

**Table (6):** Maximum Error in Paper results in Comparison with an FEM analysis.

$r$	Flexural Stresses Error %	Shear Stresses Error %	Deformations Error %
0.25	0.05	2.3	2.0
0.5	0.04	1.7	1.6
1.0	0.01	1.0	0.1
2.0	0.06	1.8	1.6
3.0	0.04	2.1	1.7

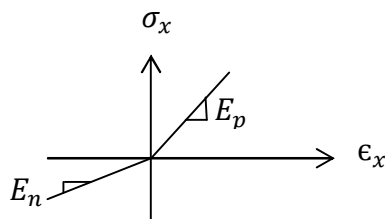


**Figure (1):** The stress strain curve for a bimodular material.

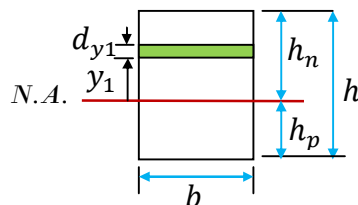


**Figure (2):** A cross section in a bimodular beam.

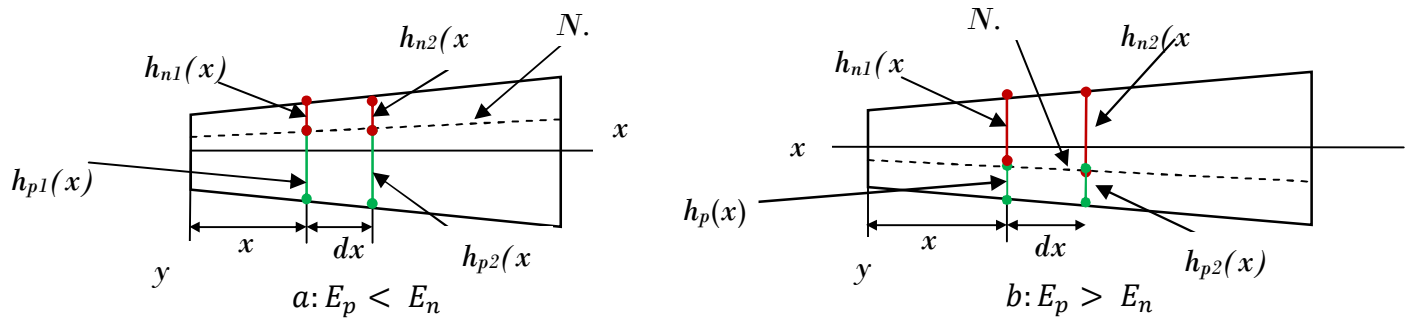


Figure (3): A Tapered bimodular beam in positive bending moment.

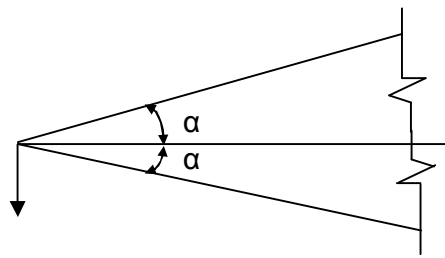


Figure (4): A wedge cantilever beam.

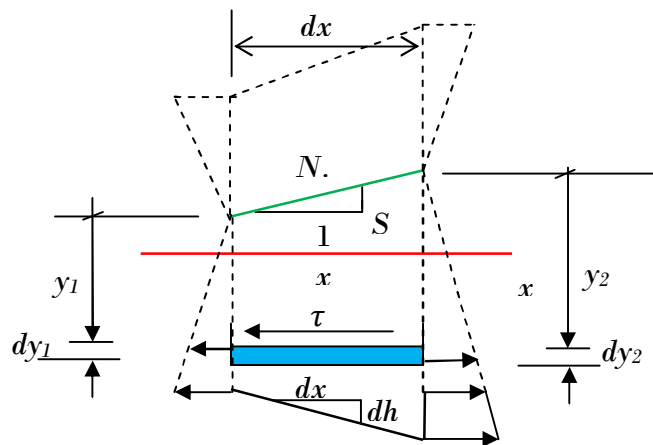


Figure (5): Shear stresses below the N.A. in an element of a bimodular beam with  $(r < 1)$  and positive bending moment.

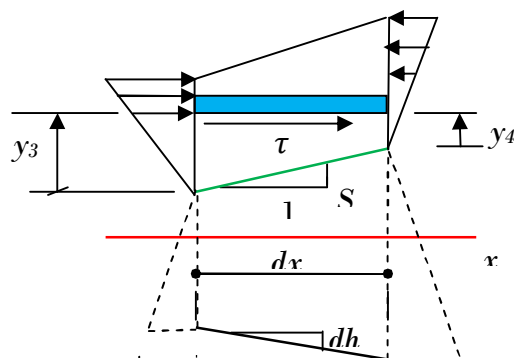


Figure (6): Shear stresses above the N.A. in an element of a bimodular beam with  $(r < 1)$  and positive bending moment.

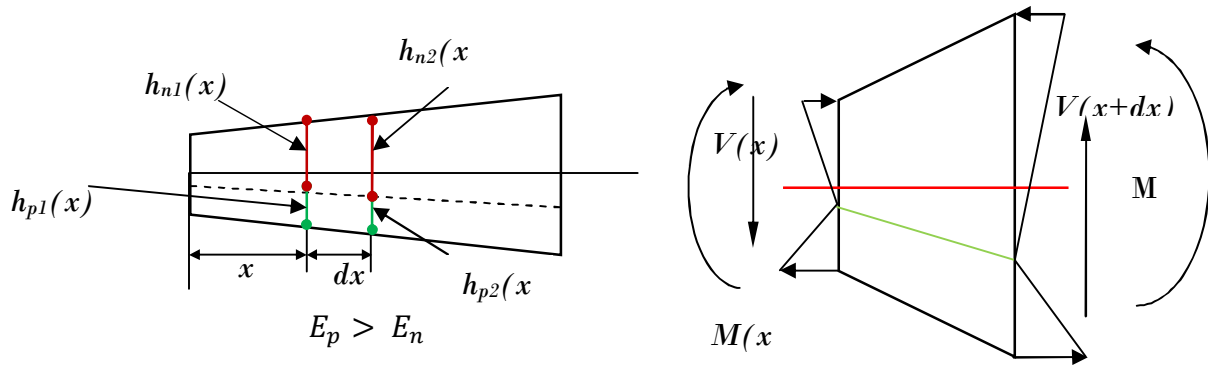


Figure (7): A Tapered bimodular beam in positive bending moment with  $(r > 1)$ .

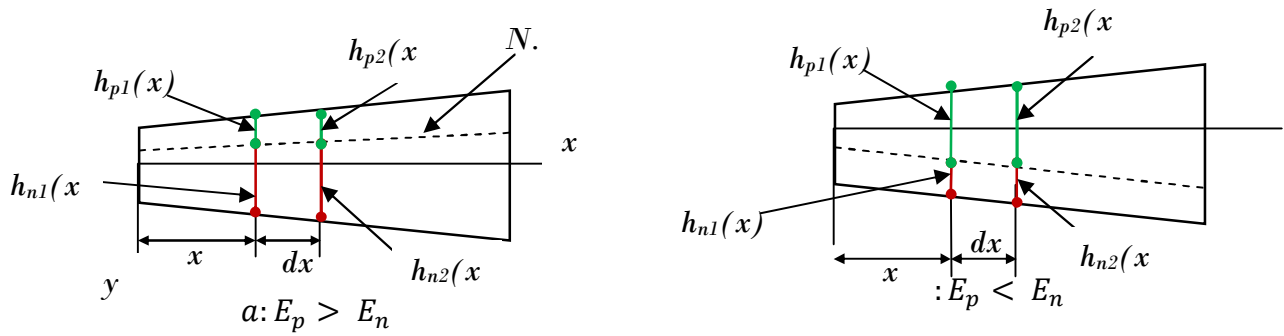


Figure (8): An element taken from a bimodular beam in Negative bending moment.

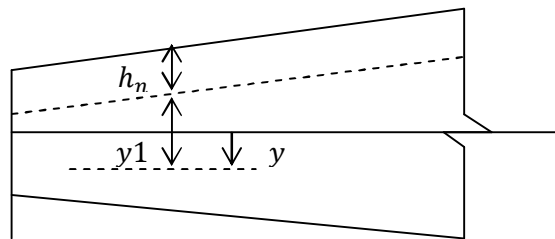


Figure (9): The transformation of the  $y$  coordinates of the N.A. and the Cartesian  $y$  coordinate for Positive moment and  $(r < 1)$ .

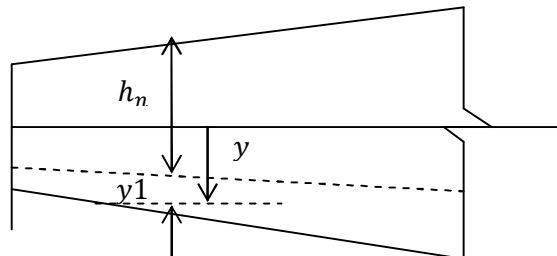
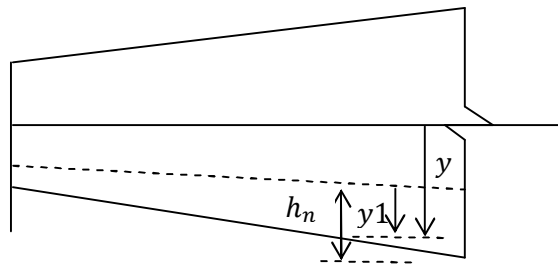
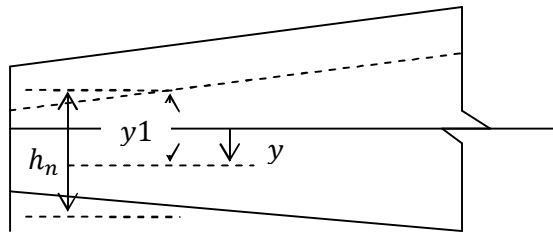


Figure (10): The transformation of the  $y$  coordinates of the N.A. and the Cartesian  $y$  coordinate for Pos. moment and  $(r > 1)$ .



**Figure (11):** The transformation of the  $y$  coordinates of the N.A. and the Cartesian coordinate for Neg. moment and ( $r < 1$ ).



**Figure (12):** The transformation of the  $y$  coordinates of the N.A. and the Cartesian  $y$  coordinate for Pos. moment and ( $r > 1$ ).

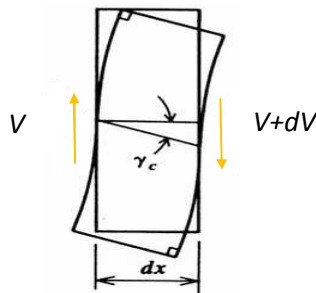


**Figure (13):** Shear stress deformations in the section of the beam.

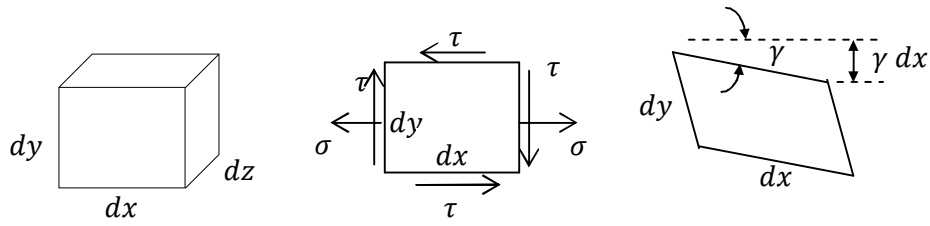


**Figure (14):** An element in a beam with flexure and shear stresses in addition to shear deformations.

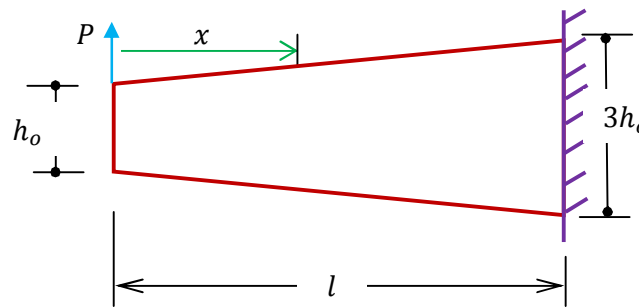
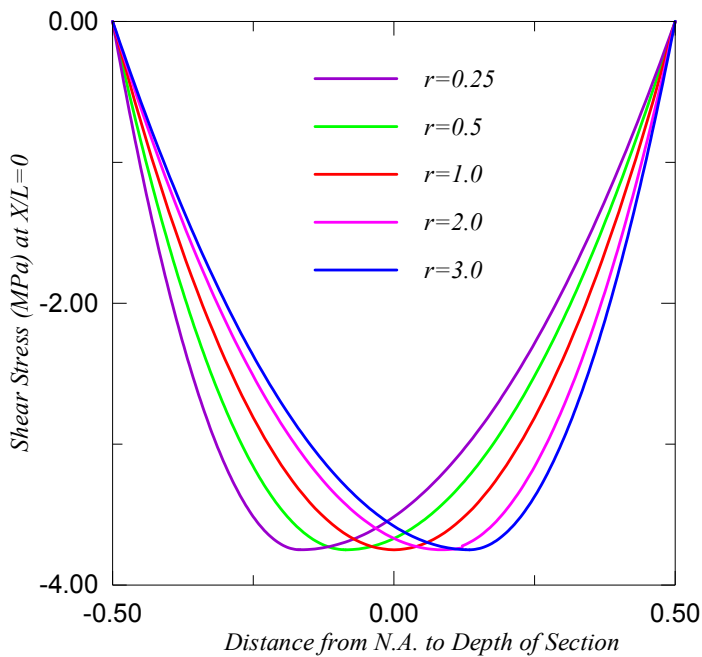


**Figure (15):** A cantilever loaded with a concentrated load at the free end.



**Figure(16):** Shear stress at the free end of beam.

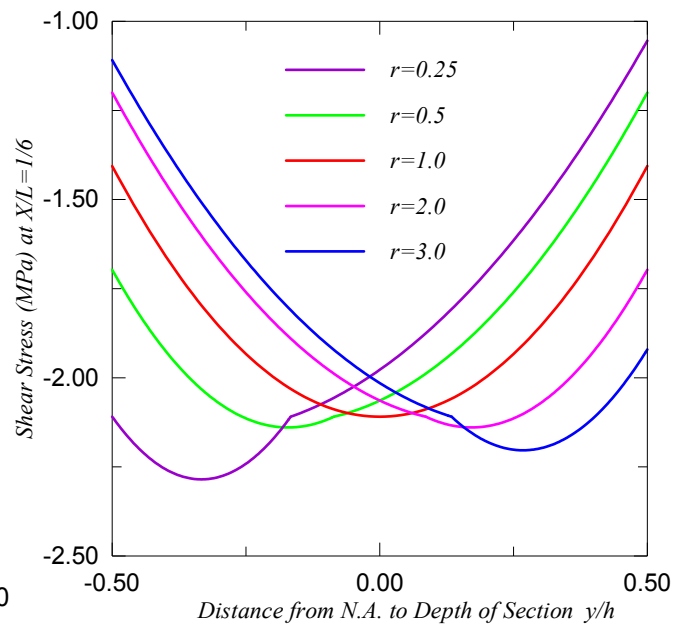


**Figure (17):** Shear stress at distance (1/6 L) from the free end of the beam.

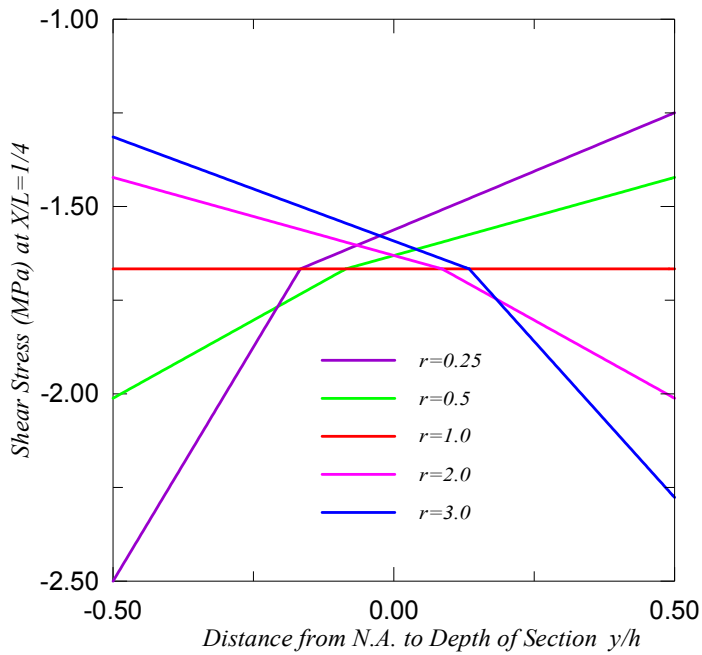


**Figure (18):** Shear stress at distance (1/4 L) from the free end of the beam.

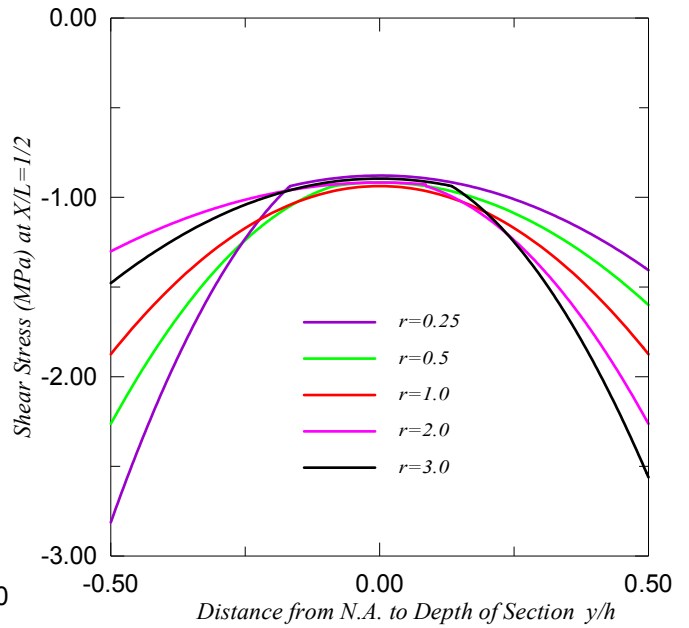


**Figure (19):** Shear stress at distance (1/2 L) from the free end of the beam.

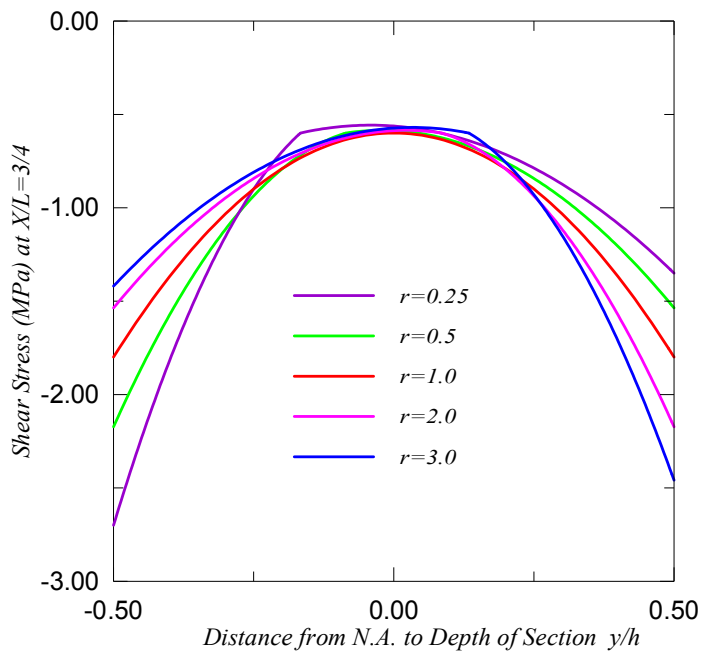


**Figure (20):** Shear stress at distance (3/4 L) from the free end of the beam.

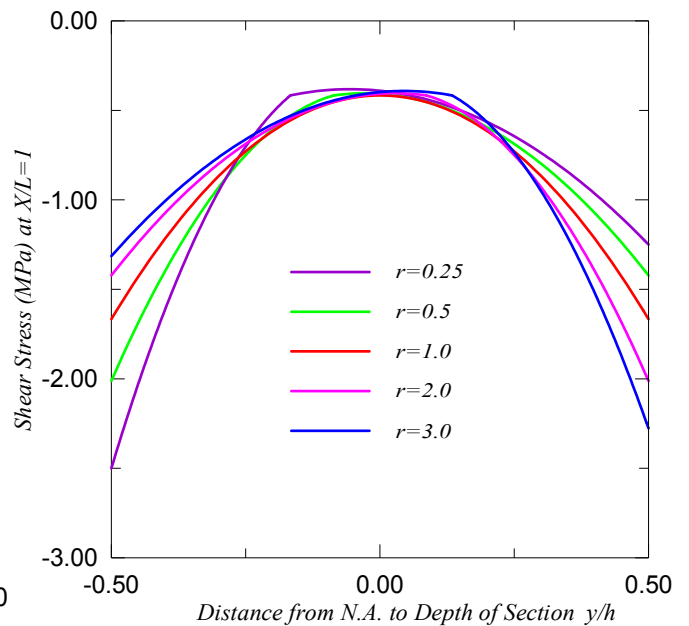


**Figure (21):** Shear stress at distance (L) from the free end of the beam.

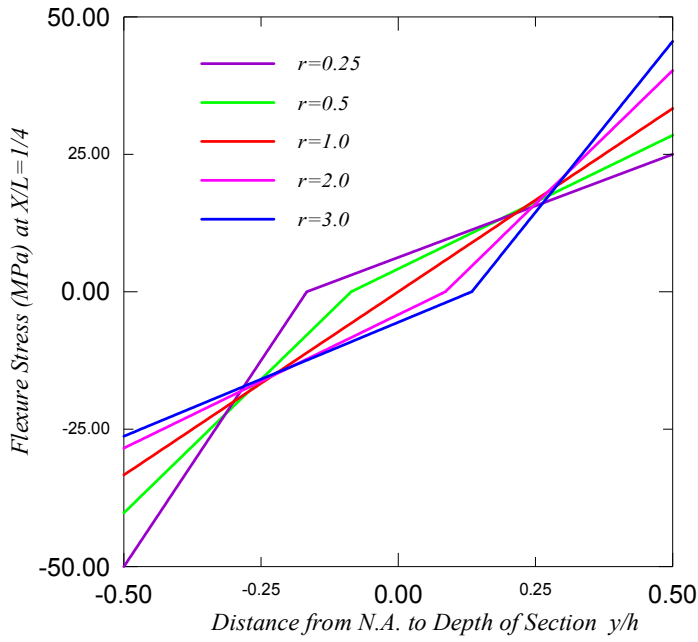


**Figure (22):** Flexure stress at distance (1/4 L) from the free end of the beam.

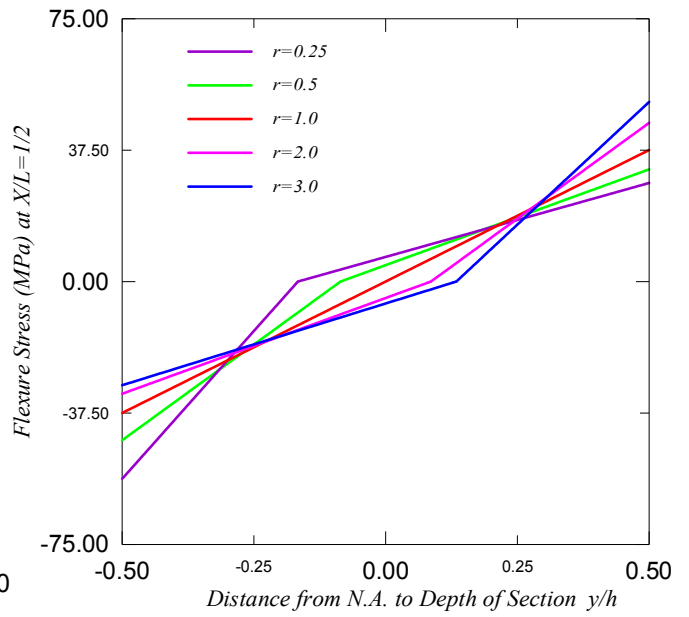


**Figure (23):** Flexure stress at distance (1/2 L) from the free end of the beam.

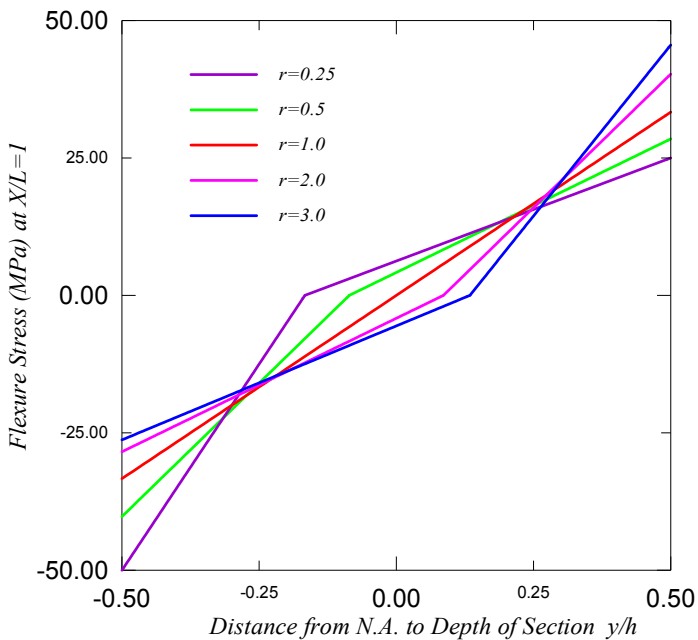


**Figure (24):** Flexure stresses at distance (L) from the free end of the beam.

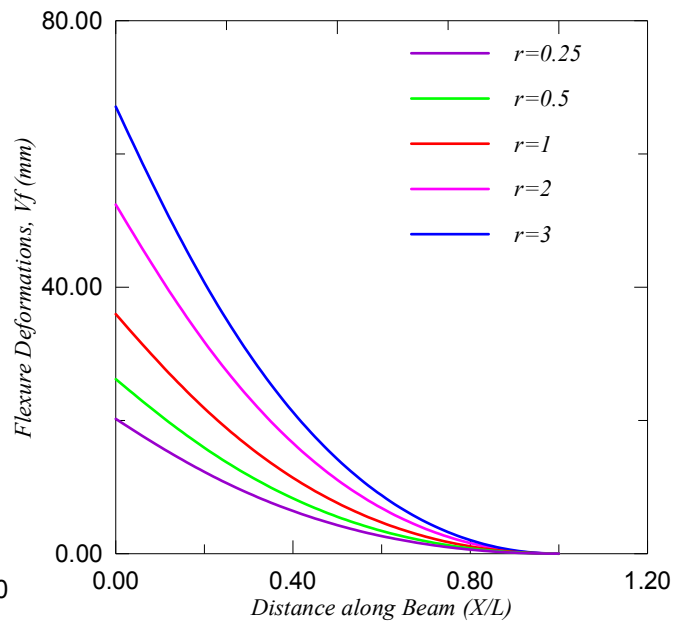


**Figure (25):** Flexure Deformations along the beam.

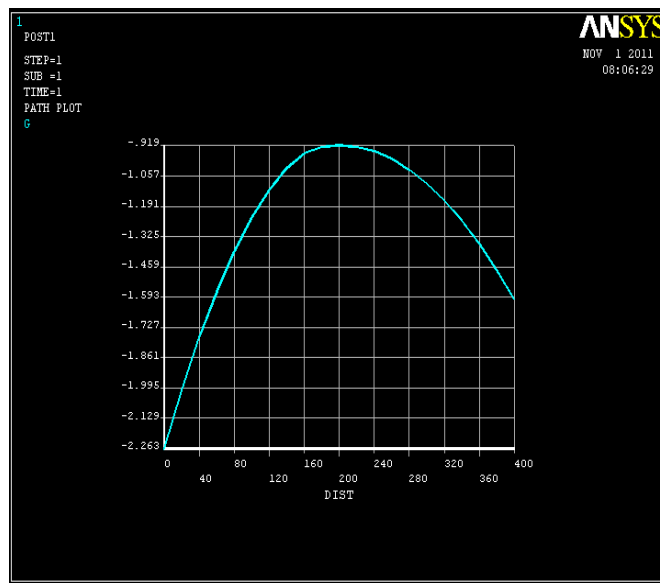
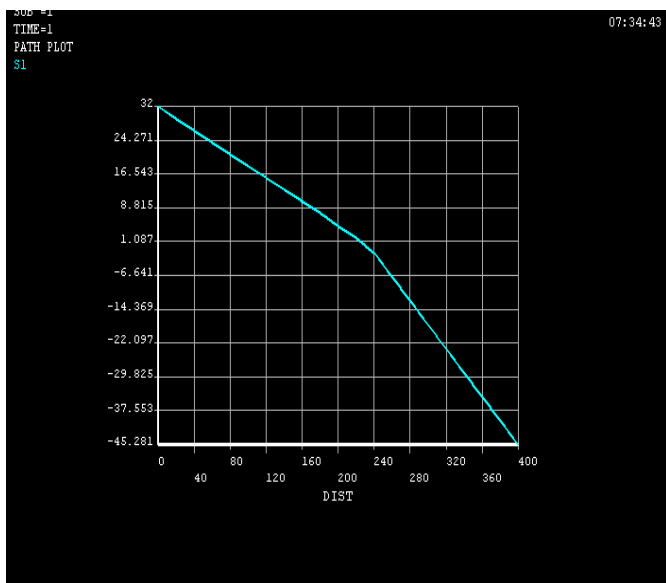


**Figure (26):** Flexural Stresses at Distance (1/2 L) from the free end ( $r=0.5$ ) (FEM Analysis with Ansys).

**Figure (27):** Shear Stresses at Distance (1/2 L) from the free end ( $r=0.5$ ) (FEM Analysis with Ansys).

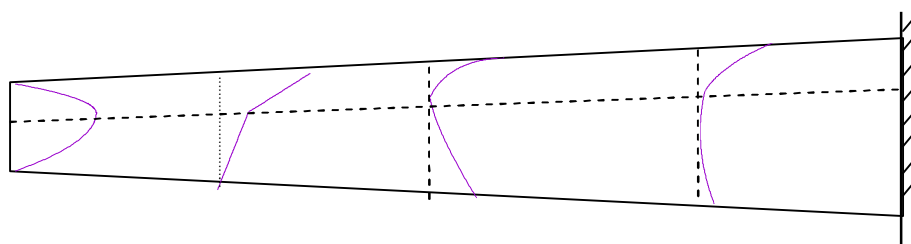


**Figure (28):** Shear stress Distributions along the Beam with ( $r=0.25$ ).

## حل تحليلي للعتبات المستدقة مزدوجة معامل المرونة

م.م. ظافر خليفة جدعان

قسم الهندسة المدنية

كلية الهندسة - جامعة الانبار

### الخلاصة

في هذا البحث طور حل للعتبات غير الموشورية المزدوجة معامل المرونة. استخدمت نظرية اويلر - برنولي مع تشوهات القص في إيجاد الحل. العتبات مزدوجة المعامل تختلف عن العتبات أحادية المعامل بكونها تمتلك معاملي مرونة احدهما للانضغاط وآخر مختلف للشد. تم تدقيق الحل بالمقارنة مع تحليل العناصر المحددة باستخدام برنامج Ansys حيث أعطى البرنامج نتائج قريبه جدا من النتائج المستحصلة من الحل المطروح في هذا البحث.

**الكلمات الرئيسية:** مستدق، غير موشوري، ثنائي معامل المرونة، عتبات.